

Topology Optimization of Thermoviscous Acoustics in Tubes and Slits with Hearing Aid Applications

R. Christensen

Hardware Platforms R&D Acoustics, GN ReSound A/S

Lautrupbjerg 7, DK-2750 Ballerup, Denmark, rechristensen@gnresound.com

Abstract: This paper describes the first ever procedure for doing topology optimization when the physics in question is thermoviscous acoustics. For now, only tubes with plane wave propagation are considered, but the topology optimization of the tube cross-section is possible for objective functions that include both viscous and thermal effects, in addition to the standard momentum and compressional effects. A condensed description of all steps from thermoviscous theory to the optimization procedure, onto the implementation in COMSOL Multiphysics, and finally to simulated and practical examples is given.

Keywords: Thermoviscous acoustics, Low Reduced Frequency, Navier-Stokes, topology optimization, transmission line parameters

Introduction

Topology optimization was first formally introduced by Bendsøe and Kikuchi in 1988 [1], with its roots in structural mechanics. The optimization process should ideally result in a design variable distribution where the corresponding material is either some reference value or void. In recent years, strategies for other physics have emerged, e.g. for acoustics [2,3]. Since acoustic topology optimization is a rather new research area, there has so far only been focus on standard acoustics, where the processes are adiabatic and reversible. However, special cases, such as thermoviscous acoustics, have yet to be investigated in the framework of topology optimization.

Thermoviscous acoustics has been a research area for the past century [4-9]. Compared to standard isentropic acoustics, where only momentum and compressional effects are considered, the effects of thermal conductivity and viscosity need to be included for accurate modelling in narrow regions, such as in hearing aid geometries, with tubes having radii in the millimeter or sub-millimeter scale. In the special case of a one-dimensional pressure field in a tube, a particular method exists for arbitrary cross-sections; this method is utilized here, since the associated equation system lends itself well to topology optimization.

Thermoviscous Acoustics

Two effects, combined denoted “thermoviscous”, are responsible for significant losses in narrow regions:

- Near a boundary with high thermal conductivity, an isothermal boundary condition is assumed. There will therefore be a thermal gradient towards the bulk, and an associated loss.
- Due to viscosity in the air, molecules will tend to stick to the boundary with a no-slip boundary condition, and this will slow down adjacent molecules. This results in a velocity gradient and added loss.

The thermoviscous behavior is illustrated in Figure 1.

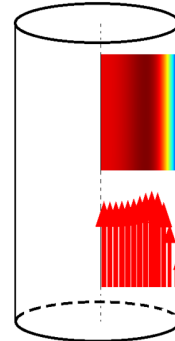


Figure 1. With isothermal/no slip conditions on the walls of a tube, the temperature variation is zero near the wall, and the velocity vectors show a different distribution near the wall compared to in the bulk.

Generally, thermoviscous acoustics is described via the so-called Full Linearized Navier-Stokes (FLNS) equation set [7] with an ideal gas assumption and for steady state behavior can be written as

$$i\omega\rho_0\vec{v} - \left(\frac{4}{3}\mu + \eta\right)\nabla \cdot (\nabla \cdot \vec{v}) + \mu\nabla \times (\nabla \times \vec{v}) + \nabla p = 0$$

$$i\omega\rho_0 C_p T - \kappa\Delta T - i\omega p = 0$$

$$\nabla \cdot \vec{v} - i\omega \frac{T}{T_0} + i\omega \frac{p}{p_0} = 0$$

where p is the pressure, T is the temperature variation, T_0 and p_0 are ambient values, ρ_0 is the density of air, \vec{v} is the velocity vector, μ is the dynamic viscosity, η is the bulk viscosity, κ is the thermal conductivity, and C_p is the specific heat at constant pressure. It is assumed that there are no sources. Appropriate boundary conditions must also be applied. The approach of solving this equation set is an option in COMSOL Multiphysics using the *Thermoviscous Acoustics* interface in the Acoustics module. The method requires a mesh, which is sufficiently fine near the boundary to capture the boundary layer effects.

Low Reduced Frequency Model

The general complexity of the FLNS method, along with the need for a refined mesh near boundaries, makes the computational cost very high for a topology optimization routine. Alternative methods exist that simplify the equation set for certain geometries, such as tubes and slits. One such method is the Low Reduced Frequency (LRF) model [6], in which it is assumed that the pressure is constant over the cross-section, and that the boundary layers are small compared to the acoustic wavelength. The model's equation system can be written in a convenient way [7,8] suited for the purpose of topology optimization. It involves solving two uncoupled 2D Helmholtz wave equations with unity source terms and complex wavenumbers:

$$\Psi_v + k_v^{-2} \Delta_{cd} \Psi_v = 1$$

and

$$\Psi_h + k_h^{-2} \Delta_{cd} \Psi_h = 1$$

where Δ_{cd} is the Laplacian in the cross-sectional directions, and with the following boundary conditions [8]

$$\Psi_v = 0 \text{ for no-slip BC}$$

$$\nabla_n \Psi_v = 0 \text{ for slip BC}$$

and

$$\Psi_h = 0 \text{ for isothermal BC}$$

$$\nabla_n \Psi_h = 0 \text{ for adiabatic BC}$$

Here, Ψ_v is a complex scalar field that describes the viscous effects, and Ψ_h is a complex scalar field that describes the thermal effects, with wavenumbers

$$k_v = \sqrt{-\omega \rho_0 / \mu}$$

and

$$k_h = \sqrt{-\omega \rho_0 C_p / \kappa}$$

These wavenumbers contain both real and imaginary parts to account for the dissipative fields.

Transmission Line Parameters

A complex and frequency-dependent density and a ditto bulk modulus can be calculated from the Ψ -fields as [9]

$$\rho = \frac{\rho_0}{\frac{1}{\Omega_{cd}} \int_{\Omega_{cd}} \Psi_v d\Omega_{cd}}$$

and

$$K = \frac{K_0}{\gamma - (\gamma - 1) \frac{1}{\Omega_{cd}} \int_{\Omega_{cd}} \Psi_h d\Omega_{cd}}$$

where ρ_0 and K_0 are the isentropic values, γ is the ratio of specific heats, and Ω_{cd} is the cross-sectional area. The density and bulk modulus can be used in a standard acoustics Helmholtz wave equation, so that thermoviscous effects are implicitly, but accurately, included. However, in the current work we will focus on the complex density and bulk modulus on their own, as these variables can be directly associated with transmission line parameters. These parameters completely describe the acoustic 1D-behavior in tubes and slits. The acoustic series impedance Z' and the acoustic shunt admittance Y' are linked to the complex density and bulk modulus as [7,9]

$$Z' \equiv R' + i\omega L' = i\omega \rho / \Omega_{cd}$$

and

$$Y' \equiv G' + i\omega C' = i\omega \Omega_{cd} / K$$

where R' is the viscous series resistance, L' is the series inertance, G' is the inverse of the thermal shunt resistance, and C' is the shunt compliance. All primed parameters are per length unit, and R', L', G' and C' are all real valued.

Topology Optimization

Topology optimization deals with solving a problem of the form [10]

$$\begin{aligned} \min_{\xi} &: \Phi(\xi, \Psi_\phi) \\ \text{s. t.} &: 0 < \xi(x, y) \leq 1 \quad \forall (x, y) \in \Omega_{cd} \\ &: \int_{\Omega_{cd}} \xi d\Omega_{cd} \leq \beta \Omega_{cd} \end{aligned}$$

where Φ is the objective function, ξ is the design variable that determines the material distribution, the Ψ_ϕ -field is the state variable, and β is maximum area fraction, to put a limit on how much of the area can be assigned ‘solid’ properties. Additional constraints can be attached to the optimization problem. It will assumed here for clarity that the entire cross-section is available for the optimization, but in general the proposed method works also for $\Omega_{cd} = \Omega_{cd,opt} \cup \Omega_{cd,nonopt}$, where the former area is to have a material distribution via the design variable, but the latter is fixed to be air with appropriate boundary conditions.

Thermovisco-acoustic topology optimization has not yet received any attention in the literature. There is no agreed upon material interpolation scheme for the FLNS model, and when interfaces between air and solid appear in during the optimization, the mesh must be able to capture the high gradient behavior, which adds to the complexity. However, with the LRF model it is possible to establish a relatively simple interpolation scheme for distributing the design variables in an optimized manner.

Design Variable Interpolation

The PDEs are written in a slightly more general form

$$a_\phi \Psi_\phi - c_\phi \Delta_{cd} \Psi_\phi = f_\phi$$

where the subscript “ ϕ ” means “either h or v”. The diffusion coefficient c_ϕ is equal to $-k_\phi^{-2}$, a_ϕ is the absorption coefficient, and f_ϕ is the source term. The letters a, c and f are chosen because of the same notation being used in the COMSOL Multiphysics PDE interface in the *Mathematics* module.

From the description of the thermoviscous method it can be seen that for typical isothermal, no-slip conditions, the Ψ -fields will be 0 on the boundary and 1 in the bulk. Hence, a heuristic approach has been taken to establish an interpolation scheme by considering that for an “air-like” material with no losses, the source term should be unity, and for a “solid-like” material, the thermal and viscous fields should approach zero, which can be obtained by a zero source term, leading to

$$f_\phi = f_\phi(\xi) = \begin{cases} 1 & \text{for } \xi = 0 \text{ (Air)} \\ 0 & \text{for } \xi = 1 \text{ (Solid)} \end{cases}$$

where ξ is the design variable to be varied to find the optimized topology. In order to have the field near a boundary go sharply to zero in the “solid” domain,

the absorption term in the solid is increased by order of magnitudes compared to the unity term for the “air” domain

$$a_\phi = a_\phi(\xi) = \begin{cases} 1 & \text{for } \xi = 0 \text{ (Air)} \\ a_{\phi,max} & \text{for } \xi = 1 \text{ (Solid)} \end{cases}$$

These extreme values are shown in Figure 2 to be able to create similar fields as with homogenous Dirichlet boundary conditions.

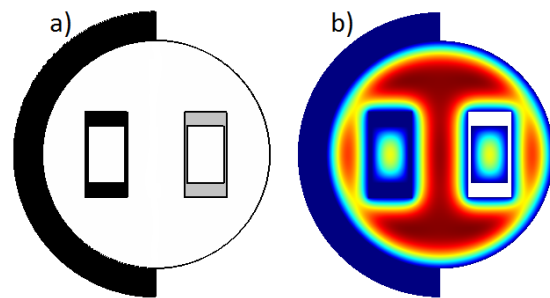


Figure 2. In a) the left half of the 2D geometry is modelled using the design variables for air (white) and solid (black), whereas the right half uses homogenous Dirichlet boundary conditions with an area removed from the simulation (grey). In b) symmetry in the field indicates valid interpolation extremes.

The intermediate values are found via the penalization schemes known as Solid Isotropic Material with Penalization (SIMP) for the source term, and Rational Approximation of Material Properties (RAMP) for the absorption coefficient, respectively, with both interpolation schemes described in [10]. We assume in this subsection that both fields follow the same interpolation, and so the subscript ϕ is removed. The SIMP interpolation scheme can then be written as

$$f(\xi) = f_{min} + \xi^{p_S}(f_{max} - f_{min})$$

for the source term, and the RAMP interpolation for the absorption term as

$$a(\xi) = a_{min} + \frac{\xi}{1 + p_R(1 - \xi)}(a_{max} - a_{min})$$

where p_S and p_R are penalty factors. Examples of these interpolation schemes are illustrated in Figure 3 and Figure 4, respectively.

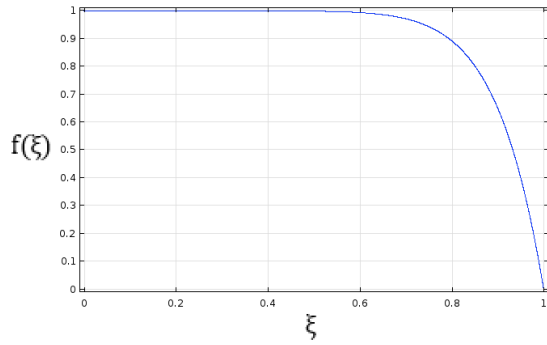


Figure 3. An example of the SIMP-interpolated source term $f(\xi)$ as a function of the design variable ξ .

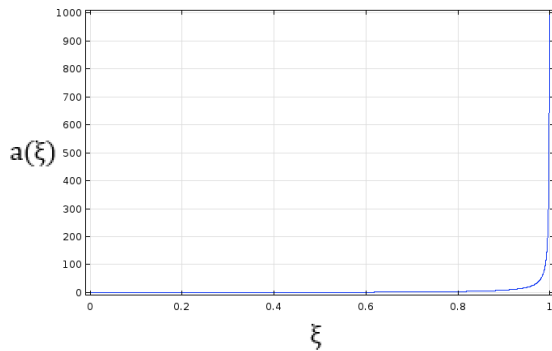


Figure 4. An example of the RAMP-interpolated absorption term $a(\xi)$ as a function of the design variable ξ .

Weak form

The harmonic PDEs can be written in weak form using the second Green's theorem, so that

$$\int_{\Omega_{cd}} a_\phi \tilde{\Psi}_\phi \Psi_\phi d\Omega_{cd} + c_\phi \int_{\Omega_{cd}} \nabla \tilde{\Psi}_\phi \cdot \nabla \Psi_\phi d\Omega_{cd} = \int_{\Omega_{cd}} \tilde{\Psi}_\phi f_\phi d\Omega_{cd} + c_\phi \int_{\partial\Omega_{cd}} \tilde{\Psi}_\phi (\nabla \Psi_\phi) \cdot \vec{n} d\partial\Omega_{cd}$$

where $\tilde{\Psi}_\phi$ is a test function. Again, remember that two equations are actually written above for $\phi = h$ and $\phi = v$, respectively.

Finite Element Discretization

For simplicity, we consider only the viscous field in the following sections. With the field being approximated via real-valued shape functions \mathbf{N} as

$$\Psi_v = \mathbf{N}^T \boldsymbol{\Psi}_v$$

and

$$\tilde{\Psi}_v = \mathbf{N}^T \tilde{\boldsymbol{\Psi}}_v$$

with $\tilde{\boldsymbol{\Psi}}_v$ being arbitrary for kinematically admissible fields, a matrix system can be set up as

$$\mathbf{S}_v \boldsymbol{\Psi}_v = \mathbf{f}_v$$

where

$$\mathbf{S}_v = \int_{\Omega_{cd}} a_v \mathbf{N} \mathbf{N}^T d\Omega_{cd} + c_v \int_{\Omega_{cd}} \nabla \mathbf{N} (\nabla \mathbf{N})^T d\Omega_{cd}$$

and

$$\mathbf{f}_v = \int_{\Omega_{cd}} \mathbf{N} f_v d\Omega_{cd} - c_v \int_{\partial\Omega_{cd}} \mathbf{N} \nabla_n \boldsymbol{\Psi}_v d\partial\Omega_{cd}$$

The integrals are evaluated numerically on an element basis, and the boundary integral is zero for slip conditions.

A more general formulation can be made which includes both the viscous field Ψ_v and the thermal field Ψ_h , but in this subsection Ψ_h is dictated by the geometry found for the optimization with only the viscous field considered.

Objective Function

Since no literature exists on the topic of topology optimization of thermoviscous acoustics, there is no typical objective function. As an example of an objective function, we seek in this subsection to maximize the viscous losses per unit length, while not changing the momentum characteristics too much, since resonances will otherwise shift in frequency. The latter is enforced via an area constraint. Only the momentum and viscous effects are considered in the optimization, and so the analysis is simplified here to reflect this, but it can be written more generally to reflect objective functions and constraints that depend on both momentum, viscous, compressional and thermal effects.

We write the viscous field objective function as

$$\max_{\xi} \Phi = \Re(R') = \Re(R'(\boldsymbol{\Psi}_v(\xi), \Omega_{cd}(\xi)))$$

where the field is implicitly a function of the design variable. It is noted, that the area of interest is only that which has air-like properties, which is different from the entire cross-sectional area; hence the area itself becomes a function of the design variable. The distribution is not binary during the optimization process, so extra measures must be taken in assessing the area. Inserting and simplifying gives the following objective function

$$\max_{\xi} \Phi = \Re(R') = \omega \rho_0 \Re \left(\frac{i}{\int_{\Omega_{cd}(\xi)} \Psi_v d\Omega_{cd}} \right)$$

with

$$\text{s. t. : } \begin{cases} 0 < \xi \leq 1 \\ \int_{\Omega_{cd}} \xi d\Omega_{cd} / \Omega_{cd} \leq \beta \\ \mathbf{S}_v \Psi_v = \mathbf{f}_v \end{cases}$$

Sensitivity Analysis

The sensitivities of the objective function to changes in the design variables are needed for the gradient-based optimization. This is done via the so-called adjoint sensitivity analysis. The procedure is described in the literature [10], and so will not be repeated here. One thing to note, however, is that the derivatives of the source term with respect to changes in the design variable need to be retained in the analysis, since this source term is a function of the design variable. This is not always the case, and so this derivative may not be included in all available literature.

Optimization Algorithm

The Method of Moving Asymptotes (MMA) [11] was used for solving the constrained optimization problem.

Regularization

A PDE density filter [12] has been applied to prevent mesh dependencies.

Implementation

The entire simulation was carried out using the Mathematics module, since all equations, including the density filter, were implemented via the *PDE* interface and the topology optimization was defined via *Optimization and Sensitivity* interface; both interfaces are in the *Mathematics* module.

There are several implications in the proposed optimization scheme compared to more traditional topology optimization. For example, cross-sectional integration has to be done over only the air domain, and so during the optimization, the structural domain must continuously be excluded. However, during the optimization process, there are regions that fall in between the two extremes, and so a logical expression is included in the integration calculation that excludes regions above a certain design variable threshold.

In order to be able capture the boundary layer effects not only on prescribed boundaries, but also at interfaces between air ($\xi=0$) and solid ($\xi=1$), a very fine mesh is applied on the entire cross-section. The computational cost of this is of little significance, since only two dimensions are considered, and only a couple of frequencies are needed to describe the behavior of the tube [8].

Simulated Results

We apply the proposed objective function of maximizing the viscous losses to a tube with a circular cross-section and no-slip/isothermal boundary conditions. The radius is 1 mm, and a single frequency of 3 kHz is examined. An area constraint of $\beta = 0.08$ is applied. The resulting optimized topology and viscous field

$$\Psi_v(\xi) = \Psi_{v,R}(\xi) + i\Psi_{v,I}(\xi)$$

are shown in Figure 5. It is observed that a “tube-in-tube” geometry has been created, with boundary layers meeting between the outer and the inner tube.

Initial conditions were that of hollow tube, i.e. the entire cross-section was assigned “air” properties. The viscous loss for the optimized geometry is approximately triple that of the initial case.

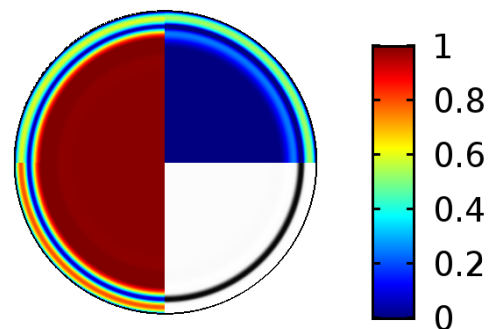


Figure 5. The viscous field $\Psi_{v,R}$ on the top left, $\Psi_{v,I}$ on the top right, absolute value of Ψ_v on the lower left, and the optimized topology on the lower right (black is solid, white is air) for a circular cross-section.

Since there are no limitations to the complexity of the cross-section, a more intricate cross-section with a small obstruction in the center, but with the same area and constraints was also investigated for the same frequency, as shown in Figure 6.

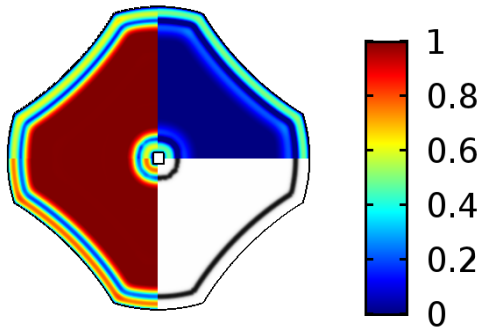


Figure 6. The viscous field $\Psi_{v,R}$ on the top left, $\Psi_{v,I}$ on the top right, absolute value of Ψ_v on the lower left, and the optimized topology on the lower right (black is solid, white is air) for a complex cross-section with both outer and inner homogenous Dirichlet boundary conditions.

It can be seen how the “solid” material is distributed near the boundaries to create high gradients in the fields; thereby giving rise to an increase in the dissipation. Similar to the circular geometry, the viscous loss per unit length for the optimized complex geometry is approximately triple that of the initial geometry.

Hearing Aid Application Example

Note: A patent application regarding a new geometry found in this section is currently in the works, and so most details regarding the geometry, the optimization procedure, and its purpose have been left out in the following description.

The topology optimization was used as part of design process for a hearing aid related case. An optimized cross-section was found, and a physical sample was made. The construction was such that a mid-section could either be empty or have the optimized geometry placed in it. At one end a so-called coupler was attached, and at the other end a printed part acts as an interface between the tube and a hearing aid receiver. The physical sample is shown in Figure 7.



Figure 7. A metal tube with an insert in the middle and a printed part at one end for receiver attachment.

The target was the pressure response in the coupler. Simulated as well as measured results are shown Figure 8.

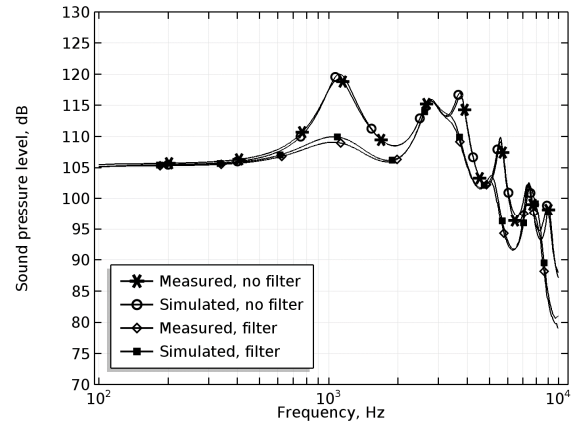


Figure 8. The measured and simulated coupler pressures, respectively, for the case with no mid-section filter, and with an optimized filter mid-section, respectively.

The optimized geometry showed good promise in the simulation with respect to the desired target, and the measurements confirmed that the responses actually were as predicted by simulations.

Discussion

In the present work only tubes have been considered, where it is assumed that the acoustic field is one-dimensional. This of course limits the applications for which the method is advantageous. On the other hand, thermoviscous effects often present themselves in relatively simple geometries with a simple pressure field, and so the proposed method will be relevant.

In the present implementation, lower-order elements are used amply to capture the boundary layer effects, but an alternative approach could be to use fewer, but higher-order elements.

It is important to realize that each optimized design is dependent on several aspects of the optimization, such as

- Choice of objective function and constraints
- Scaling of objective function and constraints
- Interpolation values and schemes
- Initial values
- Density filter radius
- Element size and distribution
- Element order of physics, optimization and filter

The acoustic pressure has only been evaluated implicitly via the velocity and thermal fields, and knowledge of the transmission line parameters' influence on the total acoustic system. An optimization with an objective function directly containing acoustic pressure should be possible, but this has not yet been investigated. The proposed topology optimization scheme can potentially be expanded to a full three-dimensional formulation.

It is desired to include an explicit length scale control, and improve the 0-1 interfaces via a projection filter scheme.

Conclusion

The current paper illustrates how COMSOL Multiphysics was used for stepping from an idea based purely on mathematics, to implementation and method testing, and onto a practical application.

A novel topology optimization scheme for thermoviscous acoustics has been presented for tube and slit structures. Each step of the procedure is outlined with some details left out. The optimization scheme has been applied to a few tube cases, where a maximization of the viscous resistance was sought, and the resulting geometries with sufficiently binary designs are shown. A practical test case illustrates the applicability of the method to general microacoustics cases.

References

1. M.P. Bendsøe, N. Kikuchi, Generating optimal topologies in structural design using a homogenization method, *Computer Methods in Applied Mechanics and Engineering*, **71**(2), 197-224 (1988)
2. M.B. Düring, J.S. Jensen and O. Sigmund, Acoustic design by topology optimization, *Journal of Sound and Vibration*, **317**, 557-575 (2008)
3. R. Christensen, How to Use Acoustic Topology Optimization in Your Simulation Studies, COMSOL blog, <https://www.comsol.dk/blogs/how-to-use-acoustic-topology-optimization-in-your-simulation-studies/>, 2016
4. G. Kirchhoff, Ueber den Einfluss der Wärmeleitung in einem Gase auf die Schallbewegung, *Ann. Phys. Chem.*, **134**, 177-193 (1868)
5. Lord Rayleigh, *The theory of sound*, Dover, New York (1945)
6. H. Tijdeman, On The Propagation of Sound Waves in Cylindrical Tubes, *Journal of Sound and Vibration*, **39**(1), 1-33 (1975)
7. M.R. Stinson, The Propagation Of Plane Sound Waves In Narrow And Wide Circular Tubes, And Generalization To Uniform Tubes Of Arbitrary Cross-Sectional Shape, *J.Acoust.Soc.Am.*, **83** (2), 550-558 (1991)
8. R. Kampinga, An Efficient Finite Element Model for Viscothermal Acoustics, *Acta Acoustica*, **97**(4), 618-631 (2011)
9. R. Christensen, Modeling the Effects of Viscosity and Thermal Conduction on Acoustic Propagation in Rigid Tubes with Various Cross-Sectional Shapes, *Acta Acoustica.*, **97**(2), 193-201 (2011)
10. M.P. Bendsøe, O. Sigmund, *Topology Optimization*, Springer, New York (2004)
11. K. Svanberg, The Method of Moving Asymptotes – A New Method for Structural Optimization, *Int. J. Numer. Methods Eng.*, **24**, 359-373, (1988)
12. B.S. Lazarov, O. Sigmund, Filters in topology optimization based on Helmholtz-type differential equations, *Int. J. Numer. Methods Eng.*, **86**(6), 765-781, (2011)

Acknowledgements

Thanks to Gojko Obradovic for several discussions regarding practical issues of small geometry acoustics. Also, thanks to Gojko again and Jan Johansen, both from GN ReSound A/S, for helping with the construction of physical samples. Finally, thanks to Junghwan Kook from GN Audio A/S for useful comments on the manuscript.